

Nonsingular Sliding Mode Guidance for Impact Time Control

Dongsoo Cho* and H. Jin Kim†

Seoul National University, Seoul 151-742, Republic of Korea
and

Min-Jea Tahk‡

Korea Advanced Institute of Science and Technology, Daejeon 305-701, Republic of Korea

DOI: 10.2514/1.G001167

A guidance problem for impact time control applicable to salvo attacks is considered based on the sliding mode control. To prevent the singularity of the guidance command, a positive continuous nonlinear function of the lead angle is introduced to the guidance command, which makes the Lyapunov stability negative-semidefinite. This issue is also resolved by the additional component of the guidance command, which makes the sliding mode be the only attractor still without the singularity. The capturability analysis is presented regardless of the initial launching conditions of missiles, which can guarantee a wide range of the capture region. The proposed guidance law is easily extended to a nonmaneuvering target using the predicted interception point. Simulation results confirm the effectiveness of the proposed guidance against a nonmaneuvering target as well as a stationary target with absence and presence of measurement noise.

I. Introduction

BASICALLY, the main objective of missiles is to effectively intercept targets with zero miss distance. To achieve this, proportional navigation guidance (PNG) has been widely studied and used for decades by the virtue of its implementation simplicity and performance effectiveness [1]. PNG law guarantees the successful interception against nonmaneuvering targets.

Recently, however, as antimissile defence systems have been developed, such as close-in weapon systems (CIWS) that take charge of detecting and destroying incoming missiles at short range, the conventional guidance law has some limitations to complete their own mission. Therefore, the tactical and advanced missile guidance is becoming the significant and essential issue such as the impact angle control guidance (IACG) and impact time control guidance (ITCG).

Because CIWS features one-to-one engagement, a salvo attack that introduces a many-to-one scenario can be a promising strategy for enhancing the survivability of missiles against the threat of CIWS. In salvo attack, multiple missiles hit the same target simultaneously. To achieve salvo attack, the impact time should be controlled for the employed multiple missiles to intercept the target at the prespecified impact time.

Although a number of papers considering IACG have been published [2–8], only a few papers related to ITCG is available in open literature. In [9], a suboptimal guidance law is proposed to control the impact time against a stationary target, which can be applied to a salvo attack of antiship missiles. The closed-form solution is a combination of the PNG and the feedback of the impact time error. In [10], the authors develop the cooperative PNG law applicable to many-to-one engagement scenarios of antiship missiles. Introducing a time-to-go variance of multiple missiles, a simultaneous attack of the missiles is achieved by decreasing the time-to-go variance cooperatively until the interception. In [11], a guidance law to control both impact time and impact angle is proposed against a stationary target, which consists of an optimal guidance law to

achieve the desired impact angle with zero miss distance and the additional term to control impact time. In [12], the authors propose a guidance law based on the differential game theory considering terminal angle and time constraints against a stationary target. In a similar way to [11], the guidance law for impact angle control is derived first in the optimal strategy and extended for both impact angle and time control by employing a time-to-go estimation. In [13], the polynomial guidance law is proposed with terminal constraints on the impact time and angle, in which the guidance command is set to be a polynomial function of the downrange-to-go with three unknown coefficients. One of the coefficients is determined to achieve the impact time requirement, and the others are determined to satisfy the terminal angle constraint and the zero miss distance.

Unlike the guidance laws in [9–13] mentioned previously, which are derived based on linearized engagement dynamics under the small angle assumption of the missile's flight-path angle, there are other guidance laws related to ITCG based on sliding mode control. In [14], a sliding-mode-control-based guidance law is proposed with the impact time and angle constraints. The desired line-of-sight angle and line-of-sight angle rate profile are defined to satisfy the requirement of the impact time and angle, then the guidance law is derived using sliding mode control to track the defined line-of-sight angle rate profile. In [15], the authors develop a guidance law for controlling the impact time using sliding mode control. In their approach, the switching surface is defined as a combination of the impact time error and the line-of-sight angle rate to meet the requirement of the impact time and zero miss distance. Using this switching surface, the guidance law is first derived for stationary targets and then extended to nonmaneuvering targets using the notion of predicted interception point. The performance of this guidance law will be compared in Sec. V with the proposed guidance law.

In this paper, a nonsingular sliding mode guidance is proposed for the impact time control against a stationary target and then extended to a nonmaneuvering target using the concept of predicted interception point motivated by [15]. However, unlike the approach in [15], the switching surface is defined as only the impact time error. The proposed guidance law is derived by enforcing the switching surface to the sliding mode for satisfying the impact time requirement. Then, to avoid the singularity of the guidance command, a positive continuous nonlinear function of the missile's lead angle is introduced to the guidance command, which results in the negative-semidefinite property of the Lyapunov stability. The problem is also resolved by the additional component, which makes the sliding mode be the only attractor. The capturability analysis shows that, regardless of the initial conditions, a wide range of the capture region can be guaranteed. In addition, we can guarantee that, on the sliding mode of the switching surface, the condition on achieving the desired impact

Received 22 November 2014; revision received 16 January 2015; accepted for publication 20 January 2015; published online 20 May 2015. Copyright © 2015 by the American Institute of Aeronautics and Astronautics, Inc. All rights reserved. Copies of this paper may be made for personal or internal use, on condition that the copier pay the \$10.00 per-copy fee to the Copyright Clearance Center, Inc., 222 Rosewood Drive, Danvers, MA 01923; include the code 1533-3884/15 and \$10.00 in correspondence with the CCC.

*Doctoral Student, School of Mechanical and Aerospace Engineering; eltrl@snu.ac.kr.

†Professor, School of Mechanical and Aerospace Engineering; hjkim@snu.ac.kr.

‡Professor, School of Aerospace Engineering; mjtahk@kaist.ac.kr.

time is a necessary and sufficient condition to the zero miss distance condition. Finally, the effectiveness of the proposed guidance law is illustrated by numerical simulations against a nonmaneuvering target as well as a stationary target through the comparison with the existing method reported in [15].

The rest of this paper is organized as follows. Section II states the engagement geometry and equation of motions. Section III describes the proposed guidance law design process with satisfying the requirement of the desired impact time. Section IV discusses the expansion of the proposed guidance law to nonmaneuvering targets. Section V shows the numerical simulation to validate the performance of the proposed control law in comparison with the existing method. Section VI describes the summary of the main results and conclusions.

II. Guidance Geometry

The missile–target planar engagement geometry is shown in Fig. 1 for a stationary target. The inertial reference frame is denoted by $X_I - O_I - Y_I$. The speed, normal acceleration, and flight-path angle are denoted by V , a , and γ ; the subscript M denotes the missile. Also, the point T means the target, r is the relative distance between the missile and target, and λ is the line-of-sight (LOS) angle. The equations of motion for missile are given by

$$\dot{x}_M = V_M \cos \gamma_M, \quad \dot{y}_M = V_M \sin \gamma_M, \quad \dot{\gamma}_M = \frac{a_M}{V_M} \quad (1)$$

Also, the engagement kinematics are expressed from Fig. 1 as

$$\dot{r} = V_r, \quad \dot{\lambda} = V_\lambda / r \quad (2)$$

where V_r and V_λ are the closing speed and the speed perpendicular to the LOS, respectively, represented as follows:

$$V_r = -V_M \cos \theta_M \quad (3)$$

$$V_\lambda = -V_M \sin \theta_M \quad (4)$$

where $\theta_M = \gamma_M - \lambda$ denotes the lead angle of the missile.

III. Impact Time Control Guidance

In this section, the sliding mode guidance law for the impact time control is derived. We define the switching surface related to the impact time constraint, then the guidance law is derived by enforcing the switching surface to the sliding mode for satisfying the impact time requirement. The proposed ITCG law is modified to avoid the singularity and includes the additional component to make the sliding mode be the only attractor. The associated stability of the proposed guidance law is analyzed using Lyapunov stability theory, and the capturability analysis is also presented.

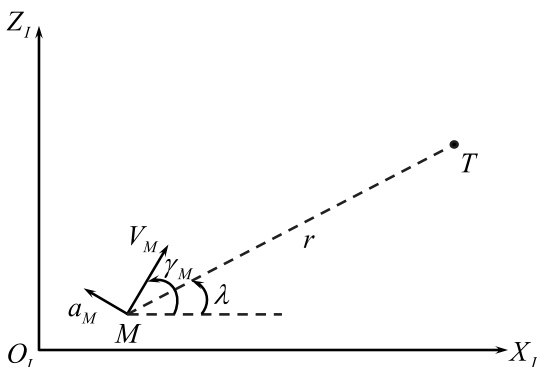


Fig. 1 Guidance geometry for a stationary target.

A. Switching Surface Design

In the engagement scenario, the impact time can be estimated as

$$t_f = t + t_{go} \quad (5)$$

where t means the elapsed time after launching an missile, and t_{go} denotes the time-to-go. For a missile to intercept a target at a desired impact time, the accurate t_{go} estimation method is essential [9,11,13,14]. In other words, the performance of the impact time guidance strongly depends on the t_{go} estimation method. For example, the conventional t_{go} estimation method (i.e., $t_{go} = -r/\dot{r}$) may produce large estimation error because the trajectory for the impact time control is curved in general, which may degrade the guidance performance [15]. In this paper, therefore, we use the improved t_{go} estimation method for stationary targets represented in [10], which is given as

$$t_{go} = \frac{r}{V_M} \left[1 + \frac{0.5}{2N-1} \theta_M^2 \right] \quad (6)$$

where $\theta_M = \gamma_M - \lambda$, and N denotes the effective navigation constant. The reason for using Eq. (6) for the time-to-go estimation will be explained in Sec. III.D.

For considering the impact time constraint, we define the following switching surface:

$$s = t_f - t_f^d = t + t_{go} - t_f^d = t_{go} - t_{go}^d \quad (7)$$

where t_{go} is represented in Eq. (6), and $t_{go}^d = t_f^d - t$ means the desired time-to-go variable, which is related to the desired impact time t_f^d . Note that the desired impact time t_f^d should be larger than r_0/V_M , where r_0 denotes the initial relative distance between the missile and the target.

Remark 1: In [15], the sliding mode guidance with the impact time constraint was also studied by defining the different switching surface given as

$$S_T = \dot{\lambda} + C s \operatorname{sign}(\dot{\lambda}) \quad (8)$$

where $s = t_{go} - t_{go}^d$, which is the same form as Eq. (7), and C is a positive constant. Their guidance law is designed to regulate S_T , not directly the impact time error s , based on Lyapunov stability theory. In this approach, it is not clearly stated in [15] how the impact time error s converges to zero for satisfying the impact time constraint, as S_T is on the sliding mode. In addition, as mentioned in [15], if $\theta_M = 0$ (i.e., $\dot{\lambda} = 0$) and $s \neq 0$, the requirement of the desired impact time cannot be satisfied with their approach. It is obvious by observing their guidance law. When $\theta_M = 0$ and $s \neq 0$, both their switching surface [Eq. (8)] and guidance law become zero. From this, the impact time error cannot be reduced. On the other hand, our approach can deal with this situation as well with satisfying the requirement of the desired impact time. The performance of the guidance law represented in [15] will be compared in Secs. V.A and V.B with the proposed ITCG law for the case when $\theta_M = 0$ and $s \neq 0$.

B. Impact Time Control Guidance Law Design

To design the guidance law for impact time control, let us consider the time derivative of the switching surface [Eq. (7)] as follows:

$$\begin{aligned} \dot{s} &= \dot{t}_{go} - \dot{t}_{go}^d \\ &= \frac{\dot{r}}{V_M} \left[1 + \frac{0.5}{2N-1} \theta_M^2 \right] - \frac{r \theta_M}{V_M (2N-1)} \dot{\lambda} + 1 + \frac{r \theta_M}{V_M^2 (2N-1)} a_M \end{aligned} \quad (9)$$

Based on Eq. (9), one can design the ITCG law using the Lyapunov-based nonlinear control theory as follows:

$$a_M = a_M^{\text{eq}} + a_M^{\text{con}} \quad (10)$$

where

$$a_M^{\text{eq}} = \frac{V_M^2(2N-1)}{r} \underbrace{\frac{(\cos \theta_M - 1)}{\theta_M}}_{T_a} + \frac{0.5V_M^2}{r} \theta_M \cos \theta_M + V_M \dot{\lambda} \quad (11)$$

$$a_M^{\text{con}} = -\frac{k}{\theta_M} s \left(\text{or } -\frac{M_1}{\theta_M} \text{sgn}(s) \right) \quad (12)$$

where k and M_1 are positive constants, and $\text{sgn}(\cdot)$ denotes the signum function. The equivalent control component a_M^{eq} is designed by letting $\dot{s} = 0$ in Eq. (9). Another control component a_M^{con} can be designed for satisfying the Lyapunov stability condition, which guarantees that the switching surface s converges to zero. The following discussion about the stability analysis and singularity is performed using the first controller in Eq. (12), i.e., $a_M^{\text{con}} = -(k/\theta_M)s$. Using the second controller in Eq. (12) with $\text{sgn}(\cdot)$, we can obtain the similar results.

Substituting Eq. (10) into Eq. (9), we obtain the following closed-loop surface dynamics

$$\dot{s} = -\frac{r}{V_M^2(2N-1)} ks \quad (13)$$

Let us consider the Lyapunov candidate function as $V = (1/2)s^2$. Then, we get

$$\dot{V} = s\dot{s} = -\frac{r}{V_M^2(2N-1)} ks^2 \quad (14)$$

From Eq. (14), we know that \dot{V} is negative-definite, and hence the condition for Lyapunov stability is satisfied.

Now, let us discuss the singularity issue of the guidance command. The guidance command [Eq. (10)] becomes singular when $r = 0$. However, technically, the interception by impact happens when $r \neq 0$ due to a certain size of the target. Therefore, the denominator r in Eq. (10) does not cause the singularity.

Another singular condition is when θ_M is equal to zero or is almost close to zero, which results in the unbounded guidance command. The first possible candidate for the singularity is the first term in Eq. (11), which is named as T_a . It seems that when $\theta_M = 0$, the term T_a becomes singular. However, by the virtue of the numerator term $(\cos \theta_M - 1)$, the term T_a forms $0/0$. Thus, to determine the limit value of T_a , we apply L'Hôpital's rule to T_a as follows:

$$\lim_{\theta_M \rightarrow 0} \frac{\cos \theta_M - 1}{\theta_M} = \lim_{\theta_M \rightarrow 0} \frac{-\sin \theta_M}{1} = 0 \quad (15)$$

From Eq. (15), we can know that the term T_a does not cause the singularity when $\theta_M = 0$.

Another possible candidate for the singularity is the control component a_M^{con} in Eq. (12). To check the existence of the singularity of this term, we consider the singularity conditions divided by two cases in the following:

$$\text{Case 1: } \theta_M = 0 \text{ and } s = 0, \quad \text{Case 2: } \theta_M = 0 \text{ and } s \neq 0 \quad (16)$$

In case 1, the control component a_M^{con} forms $0/0$. Thus, similarly to Eq. (15), applying L'Hôpital's rule to a_M^{con} yields

$$\lim_{\theta_M \rightarrow 0} \frac{s}{\theta_M} = \lim_{\theta_M \rightarrow 0} \frac{\dot{s}}{\dot{\theta}_M} = \lim_{\theta_M \rightarrow 0} \frac{\dot{s}}{\dot{\gamma}_M - \dot{\lambda}} \quad (17)$$

where \dot{s} is represented in Eq. (13). In addition, from Eqs. (1), (4), (10), and (11), the condition $\theta_M = 0$ leads to the following results:

$$\dot{\lambda} = 0, \quad a_M^{\text{eq}} = 0, \quad \dot{\gamma}_M = \frac{a_M^{\text{con}}}{V_M} = -\frac{k}{V_M \theta_M} s \quad (18)$$

Substituting Eqs. (13) and (18) into Eq. (17), we obtain

$$\lim_{\theta_M \rightarrow 0} \frac{s}{\theta_M} = \lim_{\theta_M \rightarrow 0} \frac{r\theta_M}{V_M(2N-1)} = 0 \quad (19)$$

From Eqs. (15) and (19), it implies that the guidance command [Eq. (10)] does not have the singularity problem in the desired steady state (i.e., $\theta_M = 0$) and $s = 0$.

On the other hand, in case 2 of Eq. (16), the control component a_M^{con} makes the guidance command singular. To avoid this singularity problem, the guidance command [Eq. (10)] is modified as follows:

$$a_M = a_M^{\text{Mcon}} + a_M^{\text{eq}} \quad (20)$$

where the equivalent control component a_M^{eq} is selected identically to Eq. (11), and

$$a_M^{\text{Mcon}} = -\frac{h(\theta_M)}{\theta_M} ks \quad (21)$$

Here, we introduce the continuous positive function $h(\theta_M)$ defined as

$$h(\theta_M) = \begin{cases} \frac{\text{sgn}(\theta_M)\theta_M}{\epsilon_2 - \epsilon_1} & \text{if } |\theta_M| < \epsilon_1 \\ \frac{1 - \epsilon_1}{\epsilon_2 - \epsilon_1} |\theta_M| + \frac{\epsilon_1(\epsilon_2 - 1)}{\epsilon_2 - \epsilon_1} & \text{if } \epsilon_1 \leq |\theta_M| \leq \epsilon_2 \\ 1 & \text{otherwise} \end{cases} \quad (22)$$

where ϵ_1 and ϵ_2 are small positive constants. From the property of $h(\theta_M)$, in the singular region (i.e., $|\theta_M| < \epsilon_0$, where $\epsilon_0 < \epsilon_1$), the modified control component [Eq. (21)] becomes $a_M^{\text{Mcon}} = -\text{sgn}(\theta_M)ks$, which is not singular.

Next, the stability associated with the modified guidance command [Eq. (20)] is analyzed. Similarly to Eqs. (13) and (14), using the Lyapunov candidate function, we obtain

$$\dot{V} = s\dot{s} = -\frac{rh(\theta_M)}{V_M^2(2N-1)} ks^2 \quad (23)$$

Here, another problem also remains (i.e., \dot{V} is negative-semidefinite), which implies that the sliding mode $s = 0$ cannot be achieved when $\theta_M = 0$. In other words, the modified guidance command [Eq. (20)] does not have the singularity problem but cannot satisfy the impact time constraint when $\theta_M = 0$ and $s \neq 0$.

To resolve this problem, we add a new term named as a_M^{sw} to Eq. (20) as follows:

$$a_M = a_M^{\text{Mcon}} + a_M^{\text{eq}} + a_M^{\text{sw}} \quad (24)$$

where a_M^{eq} and a_M^{Mcon} are identically designed as in Eqs. (11) and (21), respectively, and

$$a_M^{\text{sw}} = -M(p \text{sgn}(\theta_M) + 1) \text{sgn}(s) \quad (25)$$

where $p > 1$ and $M > 0$. The guidance command [Eq. (24)] is the final version of the proposed ITCG law in this paper.

Similarly to Eq. (23), the associated stability analysis of the proposed ITCG law [Eq. (24)] is summarized as follows:

$$\dot{V} = s\dot{s} = -\frac{rh(\theta_M)}{V_M^2(2N-1)} ks^2 - \frac{Mr}{V_M^2(2N-1)} (p|\theta_M| + \theta_M)|s| \quad (26)$$

where $(p|\theta_M| + \theta_M) \geq 0$. From Eq. (26), it seems that \dot{V} is negative-semidefinite, which implies that the sliding mode $s = 0$ cannot be fulfilled when $\theta_M = 0$. To achieve the sliding mode $s = 0$, it is

necessary to show that $\theta_M = 0$ is not an attractor. To show this, let us consider the dynamics of θ_M as follows:

$$\dot{\theta}_M = \dot{\gamma}_M - \dot{\lambda} \quad (27)$$

Similarly to Eq. (18), when $\theta_M = 0$, from Eqs. (21), (24), and (25), we can obtain the following results:

$$\dot{\lambda} = 0, \quad a_M^{\text{eq}} = 0, \quad a_M^{\text{Mcon}} = 0, \quad \dot{\gamma}_M = \frac{a_M^{\text{sw}}}{V_M} = -\frac{M}{V_M} \text{sgn}(s) \quad (28)$$

Substituting Eq. (28) into Eq. (27) yields

$$\dot{\theta}_M = -\frac{M}{V_M} \text{sgn}(s) \quad (29)$$

From Eq. (29), when $\theta_M = 0$ and $s \neq 0$, we know $\dot{\theta}_M \neq 0$, which implies that $\theta_M = 0$ is not an attractor. For $\theta_M \neq 0$ ($h(\theta_M) > 0$), the Lyapunov stability condition is already proven by Eq. (26). This is the main objective of a_M^{sw} represented in Eq. (25). Finally, $\theta_M = 0$ becomes an attractor just for $\theta_M = 0$ and $s = 0$, which is the achieved steady state. Therefore, the proposed ITCG law [Eq. (24)] can intercept the target without any singularity problem even though $\theta_M = 0$ at the desired impact time.

C. Capturability Analysis

This subsection performs the capturability analysis of the proposed guidance law. From Eq. (26), we have already proven that the switching surface s converges to zero. Then, when $s = 0$, from Eqs. (6) and (7), we can obtain the following relation:

$$t_{\text{go}} = \frac{r}{V_M} \left[1 + \frac{0.5}{2N-1} \theta_M^2 \right] = t_{\text{go}}^d \quad (30)$$

where $t_{\text{go}}^d = t_f^d - t$. As the elapsed time t increases, the term t_{go}^d decreases, which shows using Eq. (30) that the relative distance r also decreases. Finally, when t_{go}^d goes to zero, the relative distance r also goes to zero, which implies that the missile can capture the target at the desired impact time. On the sliding mode $s = 0$ under our proposed approach, the impact time condition $t = t_f^d$ is a necessary and sufficient condition for the zero miss distance condition $r = 0$. Because this relationship holds if $s = 0$ regardless of the initial condition, the proposed approach can guarantee a wide range of the capture region.

D. Relation Between Proportional Navigation Guidance and Proposed Impact Time Control Guidance Law

In this paper, we used the time-to-go estimation method [Eq. (6)] proposed in [10]. In [10], the time-to-go estimation is derived under the assumption that the guidance command forms the PNG law with the small angle approximation. To obtain the validity of use of Eq. (6) in our approach, it is necessary to show that the proposed ITCG law finally forms the PNG law. To show this, we apply the small angle approximation with respect to θ_M as

$$\cos \theta_M \approx 1 - \frac{1}{2} \theta_M^2, \quad \sin \theta_M \approx \theta_M \quad (31)$$

where the third-order term $\mathcal{O}(\theta_M^3)$ is negligible.

After the sliding mode $s = 0$ occurs with Eq. (31), the proposed ITCG law [Eq. (32)] is reduced to

$$a_M \approx -\frac{V_M^2(2N-1)}{2r} \theta_M + \frac{0.5V_M^2}{r} \theta_M + V_M \dot{\lambda} \approx NV_M \dot{\lambda} \quad (32)$$

where $\dot{\lambda} \approx (-1/r)V_M \theta_M$ from Eqs. (4) and (31). Therefore, the proposed guidance law forms the PNG law after occurrence of the sliding mode.

E. Summary of Proposed Impact Time Control Guidance Law

To summarize, the proposed ITCG law is designed as follows:

$$a_M = a_M^{\text{eq}} + a_M^{\text{Mcon}} + a_M^{\text{sw}} \quad (33)$$

where

$$a_M^{\text{eq}} = \frac{V_M^2(2N-1)}{r} \underbrace{\frac{(\cos \theta_M - 1)}{\theta_M}}_{T_a} + \frac{0.5V_M^2}{r} \theta_M \cos \theta_M + V_M \dot{\lambda} \quad (34)$$

$$a_M^{\text{Mcon}} = -\frac{h(\theta_M)}{\theta_M} ks, \quad h(\theta_M) = \begin{cases} \text{sgn}(\theta_M) \theta_M & \text{if } |\theta_M| < \epsilon_1 \\ \frac{1-\epsilon_1}{\epsilon_2-\epsilon_1} |\theta_M| + \frac{\epsilon_1(\epsilon_2-1)}{\epsilon_2-\epsilon_1} & \text{if } \epsilon_1 \leq |\theta_M| \leq \epsilon_2 \\ 1 & \text{otherwise} \end{cases} \quad (35)$$

$$a_M^{\text{sw}} = -M(p \text{sgn}(\theta_M) + 1) \text{sgn}(s) \quad (36)$$

where $\epsilon_2 > \epsilon_1 > 0$, $p > 1$, and $k, M > 0$. On the singular point $\theta_M = 0$, the term T_a in Eq. (34) becomes zero from Eq. (15). The objective of $h(\theta_M)$ in Eq. (35) is to avoid the singularity in the modified control component a_M^{Mcon} (when $\theta_M = 0$, $a_M^{\text{Mcon}} = 0$). Because of the existence of $h(\theta_M)$, the derivative of the Lyapunov candidate function is negative-semidefinite from Eq. (26), which cannot prove the convergence to the sliding mode $s = 0$ when $\theta_M = 0$ and $s \neq 0$. To resolve this problem, the new component a_M^{sw} represented in Eq. (36) is added, which guarantees that $\theta_M = 0$ is not an attractor when $s \neq 0$ from Eq. (29).

IV. Expansion to Nonmaneuvering Targets

In this section, the proposed ITCG law is easily extended to a nonmaneuvering target using the predicted interception point (PIP) represented in [15]. Because the target is nonmaneuvering, the PIP can be defined as a fixed point where the missile is expected to intercept the target at the desired impact time. However, if there exists an impact time error, the fixed PIP may lead to a large miss distance and degrade the guidance performance [15]. To avoid this problem, as shown in Fig. 2, the PIP, $T_P = (x_{TP}, y_{TP})$, is defined as a time-varying point, which is updated as follows:

$$x_{TP} = x_T + [V_T \cos \gamma_T] t_{\text{go}}, \quad y_{TP} = y_T + [V_T \sin \gamma_T] t_{\text{go}} \quad (37)$$

where t_{go} is the time-to-go estimate for a stationary target defined in Eq. (6). Using the PIP, we can deal with a nonmaneuvering target as a virtual stationary target. From this, the direct t_{go} estimation method for a nonmaneuvering target is not required, which is the advantage of PIP. The expansion of the proposed ITCG law derived in Sec. III.B to a nonmaneuvering target can be easily performed just by replacing r and λ with r_P and λ_P , respectively.

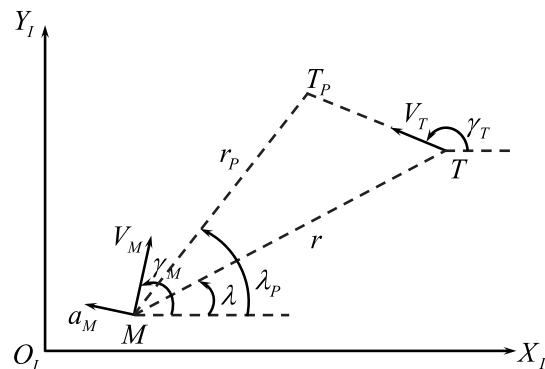


Fig. 2 Guidance geometry for a nonmaneuvering target using PIP.

Table 1 Simulation parameters for scenario 1 and 2

Parameters	Scenario 1	Scenario 2
Initial missile position	(0,0) km	
Missile velocity	250 m/s	
Initial missile flight-path angle	0 deg	
Initial target position, km	(10,0)	(7,0)
Target velocity	—	100 m/s
Initial target flight-path angle	—	0 deg
Desired impact time	50 ~ 110 s	
Proposed ITCG gains	$k = 50, M = 10, p = 2,$ $\epsilon_1 = 0.001, \epsilon_2 = 0.015$	

V. Simulation Results

This section illustrates the effectiveness of the proposed ITCG law for the impact time constraint via numerical simulation. In Sec. V.A, we perform the simulation against a stationary target. In Sec. V.B, the proposed approach is extended to a nonmaneuvering target using the predicted interception point (PIP) concept represented in [15]. In both subsections, we compare the proposed ITCG law with the existing guidance law named as SMG represented in [15]. In Sec. V.C, the performance of the proposed ITCG is evaluated by Monte Carlo simulation to analyze the effect of measurement noise against a nonmaneuvering target.

To avoid the chattering for implementation of the proposed ITCG law, only the signum function $\text{sgn}(\cdot)$ in Eq. (36), which is the discontinuous component, is approximated by the sigmoid function given as [8]

$$\text{sgmf}(z) = 2 \left(\frac{1}{1 + \exp^{-\alpha z}} - \frac{1}{2} \right), \quad \alpha > 0 \quad (38)$$

where α is chosen as 20. In addition, the maximum limit of the missile acceleration command is chosen as $10g$, where $g = 9.81 \text{ m/s}^2$.

All simulations are terminated when the relative distance r is less than 0.3 m. We use the same controller gains of the proposed guidance law listed in Table 1 for all cases of engagement scenarios studied in this paper.

A. Scenario 1: Against a Stationary Target

This subsection shows the performance of the proposed ITCG law against a stationary target. For the performance comparison, we also simulated another guidance law, SMG represented in [15]. The simulation parameters used in scenario 1 are listed in Table 1.

Figure 3 represents the simulation results of scenario 1. Figures 3a–3d show the missile trajectory, guidance command, impact time error, and lead angle, respectively, at the different desired impact times. As listed in Table 1, the initial conditions of scenario 1 are $\gamma_M(0) = 0$ and $\lambda(0) = 0$, which means that the initial lead angle $\theta_M(0)$ is also zero. From this, as mentioned in remark 1, the SMG law generates zero command (see dashed line in Fig. 3b). Therefore, the missile just heads for the target (see dashed line in Fig. 3a), then finally intercepts the target at the impact time 40 s. This is clearly observed by the dashed lines in Fig. 3c ending at 40 s in spite of the different desired impact time. Thus, when $\theta_M = 0$ and $s \neq 0$, the desired impact time cannot be achieved by the SMG represented in [15].

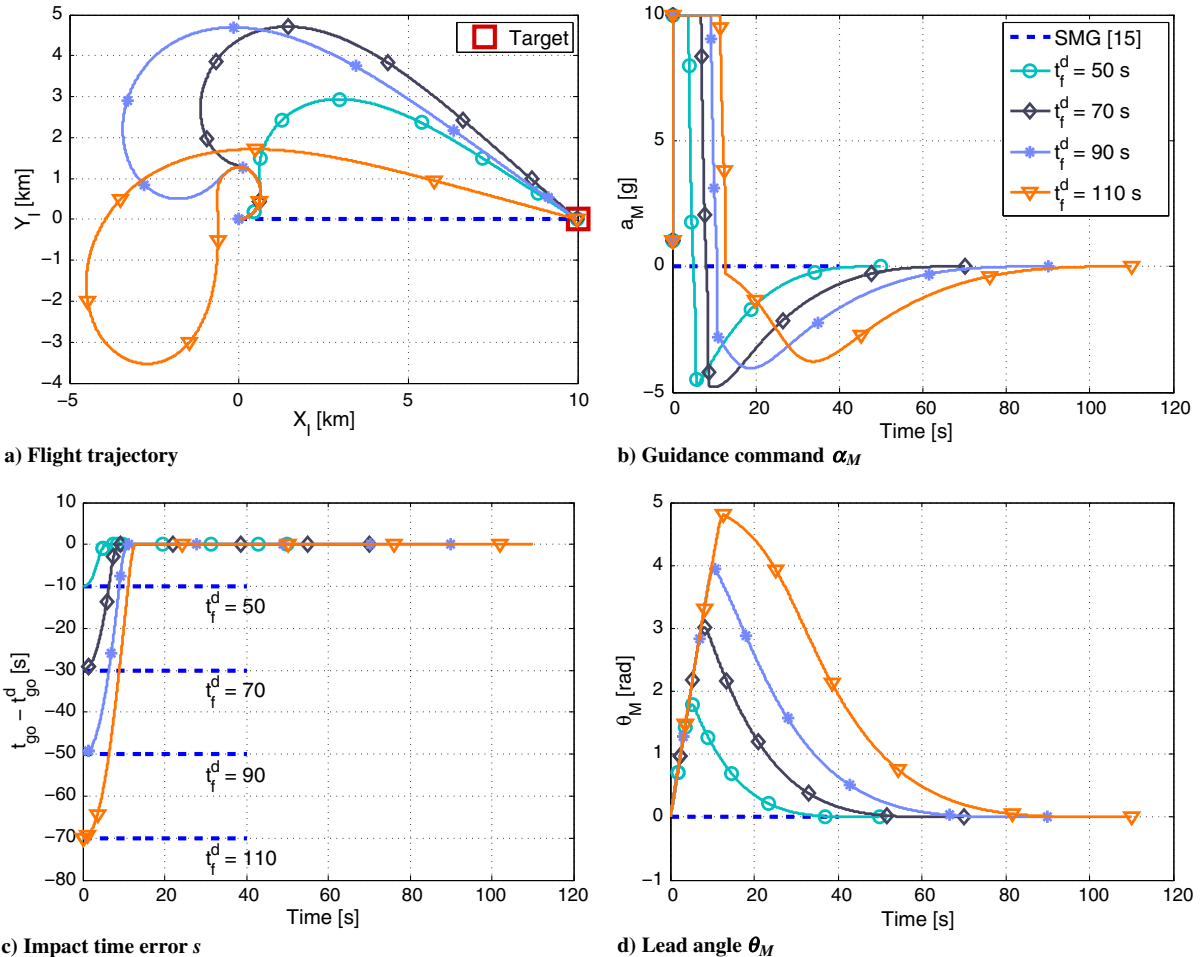


Fig. 3 Scenario 1 against a stationary target at different desired impact times: solid-patterned line represents the results of the proposed ITCG law.

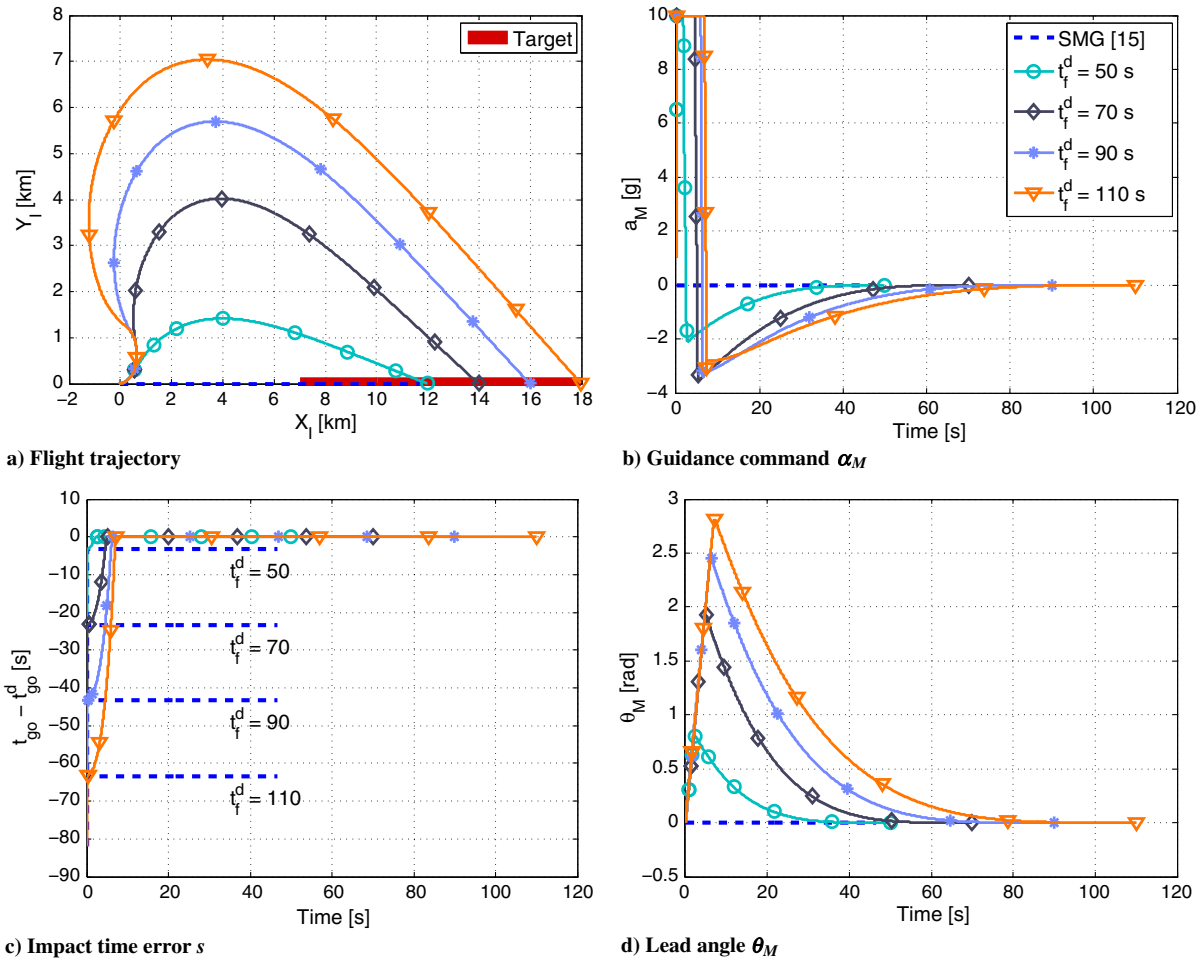


Fig. 4 Scenario 2 against a nonmaneuvering target at different desired impact times: solid-patterned line represents the results of the proposed ITCG law.

On the other hand, when $\theta_M = 0$ and $s \neq 0$, the proposed ITCG law can guarantee that the missile intercepts the target at all the desired impact times studied in scenario 1 within the final impact time error $|t_f - t_f^d| \leq 1 \times 10^{-4}$ s. These results come from the existence of a_M^{sw} represented in Eq. (36). As the desired impact time increases, the missile trajectory turns farther away from the target in the initial phase (see solid-patterned line in Fig. 3a). These results were obtained using the guidance command shown in Fig. 3b. In the initial phase, the large amplitude of the guidance command is generated to regulate the impact time error s quickly for satisfying the requirement of the different desired impact time. Furthermore, in the terminal phase, all the guidance commands converge to zero, which causes the missile to gradually approach the collision course to the target. As expected, when θ_M goes to zero as shown in Fig. 3d, the proposed ITCG law shown in Fig. 3b does not suffer from the singularity problem.

B. Scenario 2: Against a Nonmaneuvering Target

This subsection represents the performance of the proposed ITCG law against a nonmaneuvering target. The performance is also compared with the SMG law represented in [15]. Based on [15], the

proposed approach is extended to a nonmaneuvering target using the predicted interception point (PIP) discussed in Sec. IV. The initial position of the target is set on (7,0) km. In addition, the target is assumed to be moving at a velocity of 100 m/s with a flight-path angle of 0 deg. The other simulation parameters are listed in Table 1.

Similarly to scenario 1, the initial lead angle is set to $\theta_M(0) = 0$. From this, the SMG law generates zero command (see dashed line in Fig. 4b), which incurs that the missile flies toward the target (see dashed line in Fig. 4a) and intercepts the target at the impact time 46.666 s. This fact is also confirmed from the dashed line in Fig. 4c. Thus, we can conclude that, when $\theta_M = 0$ and $s \neq 0$, the SMG law cannot satisfy any desired impact time constraints.

On the other hand, the solid-patterned lines in Fig. 4 indicate that, even against a nonmaneuvering target, the proposed ITCG law still is able to intercept the target with prespecified impact time within the final impact time error $|t_f - t_f^d| \leq 1 \times 10^{-4}$ s. As shown in Fig. 4b, the initial large acceleration command is generated, then the required guidance command converges to zero. The reasons have already been discussed in Sec. V.A. As expected, even against a nonmaneuvering target, when θ_M goes to zero as shown in Fig. 4d, the singularity of the proposed ITCG law still does not appear (see solid-patterned line in Fig. 4b).

C. Salvo Attack Against a Nonmaneuvering Target in the Presence of Measurement Noise

The final simulation is performed with the proposed ITCG law for a salvo attack. The objective of scenario 3 is for four missiles, each with different initial conditions, to intercept a single nonmaneuvering target at a desired impact time. The desired impact time is specified as 60 s, each of the missiles is assumed to be moving at 250 m/s, and the target is supposed to be traveling at 150 m/s with a flight-path angle

Table 2 Simulation parameters for salvo attack

$r_f^d = 60$ s	(X_0, Y_0) , km	γ , deg
Target	(3,3)	45
Missile 1	(2,13)	90
Missile 2	(0,2)	180
Missile 3	(5,-1)	0
Missile 4	(15,15)	45

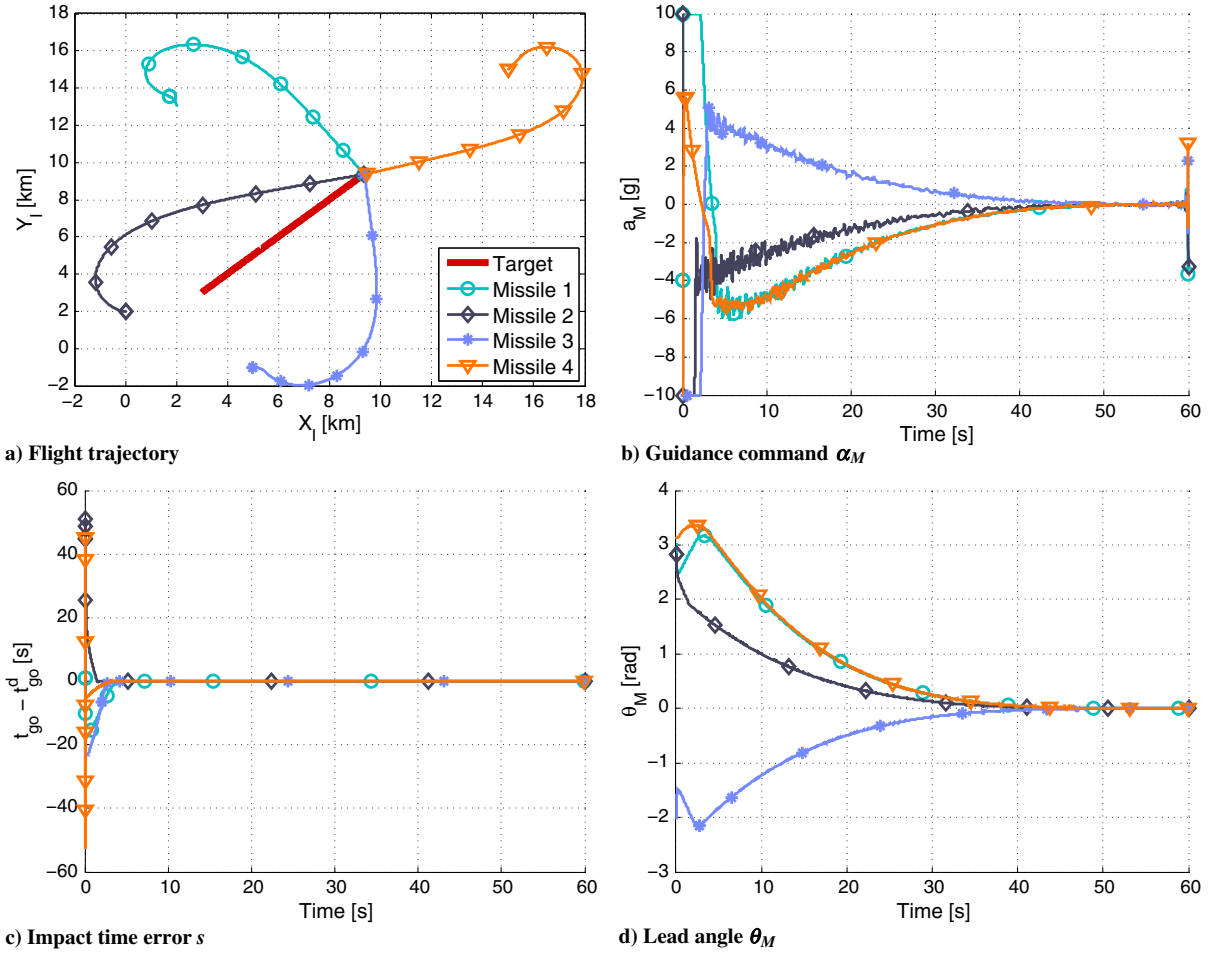


Fig. 5 Salvo attack against a nonmaneuvering target at the desired impact time of 60 s with measurement noise.

of 45 deg. The other simulation parameters are listed in Table 2, and the same gains of the proposed ITCG law are used listed in Table 1.

All the previous simulations have assumed the perfect knowledge of the measurements such as the LOS angle λ and LOS angle rate $\dot{\lambda}$. In realistic scenarios, these parameters are measured by an onboard active seeker with inherently noisy sensors. To analyze the effects of noise on the proposed ITCG law, we performed Monte Carlo simulations for each missile against a nonmaneuvering target consisting of 200 sample runs each. In these simulations, a missile seeker that measures LOS angle λ and LOS angle rate $\dot{\lambda}$ is modeled as a first-order lag system with a time constant 0.1 s subject to the additive Gaussian noise with standard deviation of 0.0175 rad ($\approx 1^\circ$). In addition, we have included the missile autopilot dynamics as a first-order lag system with a time constant 0.1 s.

Figure 5 represents a sample run of scenario 3 with the proposed ITCG law. Figure 5a shows that four missiles, with each different initial condition, successfully intercept the target at the desired impact time of 60 s even in the presence of measurement noise. For the case of missile 4, in particular, even though the missile is located in front of the target with the initial lead angle $\theta_M(0) = 0$ ($\gamma_M(0) = \lambda(0) = 45^\circ$), the target is captured at the desired impact time. The primary effect of noise is in the appearance of a chattering behavior of

the guidance command shown in Fig. 5b. From Fig. 5c, it is clearly shown that each of the missiles satisfies the desired impact time constraints.

The rms performance of Monte Carlo simulations of each missile is summarized in Table 3. From this table, four missiles can intercept the nonmaneuvering target within the miss distance $[r(t_f)]_{\text{rms}} \leq 0.170$ m and impact time error $[t_f - t_f^d]_{\text{rms}} \leq 1.19 \times 10^{-4}$ s.

VI. Conclusions

In this paper, a nonsingular sliding mode guidance is proposed for the missile to intercept the target at the desired impact time. The proposed impact time control guidance law is modified to avoid the singularity and includes the additional component to make the sliding mode be the only attractor. From the capturability analysis, regardless of the initial conditions, a wide range of the capture region can be guaranteed. Using the predicted interception point, the proposed approach is easily extended to a nonmaneuvering target with still the use of the t_{go} estimation for a stationary target. The effective performance of the proposed law is demonstrated through the numerical simulations of various engagements against stationary and nonmaneuvering targets in comparison with the existing method.

References

- [1] Zarchan, P., *Tactical and Strategic Missile Guidance*, Vol. 199, Progress in Astronautics and Aeronautics, AIAA, Reston, VA, 2002, pp. 11–29.
- [2] Kim, B. S., Lee, J. G., and Han, H. S., “Biased PNG Law for Impact with Angular Constraint,” *IEEE Transactions on Aerospace and Electronic Systems*, Vol. 34, No. 1, 1998, pp. 277–288. doi:10.1109/7.640285
- [3] Song, T. L., Shin, S. J., and Cho, H., “Impact Angle Control for Planar Engagements,” *IEEE Transactions on Aerospace and Electronic*

Table 3 RMS performance for salvo attack

$t_f^d = 60$ s	$[r(t_f)]_{\text{rms}}$, m	$[t_f - t_f^d]_{\text{rms}}$, s
Missile 1	0.165	9.68×10^{-5}
Missile 2	0.151	1.19×10^{-4}
Missile 3	0.142	1.08×10^{-4}
Missile 4	0.170	1.13×10^{-4}

- Systems*, Vol. 35, No. 4, 1999, pp. 1439–1444.
doi:10.1109/7.805460
- [4] Ryoo, C. K., Cho, H., and Tahk, M. J., “Optimal Guidance Laws with Terminal Impact Angle Constraint,” *Journal of Guidance, Control, and Dynamics*, Vol. 28, No. 4, 2005, pp. 724–732.
doi:10.2514/1.8392
- [5] Ratnoo, A., and Ghose, D., “Impact Angle Constrained Guidance Against Nonstationary Nonmaneuvering Targets,” *Journal of Guidance, Control, and Dynamics*, Vol. 33, No. 1, 2010, pp. 269–275.
doi:10.2514/1.45026
- [6] Shima, T., “Intercept-Angle Guidance,” *Journal of Guidance, Control, and Dynamics*, Vol. 34, No. 2, 2011, pp. 484–492.
doi:10.2514/1.51026
- [7] Lee, C. H., Kim, T. H., Tahk, M. J., and Whang, I. H., “Polynomial Guidance Laws Considering Terminal Impact Angle and Acceleration Constraints,” *IEEE Transactions on Aerospace and Electronic Systems*, Vol. 49, No. 1, 2013, pp. 74–92.
doi:10.1109/TAES.2013.6404092
- [8] Kumar, S. R., Rao, S., and Ghose, D., “Nonsingular Terminal Sliding Mode Guidance with Impact Angle Constraints,” *Journal of Guidance, Control, and Dynamics*, Vol. 37, No. 4, 2014, pp. 1114–1130.
doi:10.2514/1.62737
- [9] Jeon, I. S., Lee, J. I., and Tahk, M. J., “Impact-Time-Control Guidance Law for Anti-Ship Missiles,” *IEEE Transactions on Control Systems Technology*, Vol. 14, No. 2, 2006, pp. 260–266.
doi:10.1109/TCST.2005.863655
- [10] Jeon, I. S., Lee, J. I., and Tahk, M. J., “Homing Guidance Law for Cooperative Attack of Multiple Missiles,” *Journal of Guidance, Control, and Dynamics*, Vol. 33, No. 1, 2010, pp. 275–280.
doi:10.2514/1.40136
- [11] Lee, J. I., Jeon, I. S., and Tahk, M. J., “Guidance Law to Control Impact Time and Angle,” *IEEE Transactions on Aerospace and Electronic Systems*, Vol. 43, No. 1, 2007, pp. 301–310.
doi:10.1109/TAES.2007.357135
- [12] Kang, S., and Kim, H. J., “Differential Game Missile Guidance with Impact Angle and Time Constraints,” *Proceedings of the International Federation of Automatic Control World Congress*, Milano, Italy, 2011, pp. 3920–3925.
- [13] Kim, T. H., Lee, C. H., Jeon, I. S., and Tahk, M. J., “Augmented Polynomial Guidance with Impact Time and Angle Constraints,” *IEEE Transactions on Aerospace and Electronic Systems*, Vol. 49, No. 4, 2013, pp. 2806–2817.
doi:10.1109/TAES.2013.6621856
- [14] Harl, N., and Balakrishnan, S., “Impact Time and Angle Guidance with Sliding Mode Control,” *IEEE Transactions on Control Systems Technology*, Vol. 20, No. 6, 2012, pp. 1436–1449.
doi:10.1109/TCST.2011.2169795
- [15] Kumar, S. R., and Ghose, D., “Sliding Mode Control Based Guidance Law with Impact Time Constraints,” *Proceedings of American Control Conference*, Washington, D.C., June 2013, pp. 5780–5785.
doi:10.1109/ACC.2013.6580740